CHAPTER FIVE

Kinetic Analysis of the Exonuclease Activity of the Bacteriophage T4 Mre11–Rad50 Complex

Tibebe A. Teklemariam, Osvaldo D. Rivera, Scott W. Nelson[1]
Iowa State University, Ames, IA, United States
[1]Corresponding author: e-mail address: swn@iastate.edu

Contents

Abstract

Bacteriophage T4 encodes orthologs of the proteins Rad50 (gp46) and Mre11 (gp47), which form a heterotetrameric complex (MR) that is responsible for host genome degradation and the processing of DNA ends for recombination-dependent DNA repair. In this chapter, we describe the ensemble methods currently employed by our laboratory to characterize the exonuclease activity of the T4 MR complex. DNA exonucleases play a vital role in maintaining the integrity of DNA through their participation in DNA repair pathways and as proofreaders for DNA polymerases. Methods for quantifying the general features of the exonuclease, and for determining steady-state kinetic parameters (K_m, k_{cat}), the polarity of exonuclease activity, and processivity are presented. These methods should be applicable to all DNA exonucleases, and to some extent endonucleases.

Methods in Enzymology, Volume 600
ISSN 0076-6879
https://doi.org/10.1016/bs.mie.2017.12.007

ABBREVIATIONS

2AP	2-aminopurine
dsDNA	double-stranded DNA
gp46	T4 Rad50
gp47	T4 Mre11
HDR	homology-directed repair
PEI	polyethyleneimine
sDNA	single-stranded DNA
TLC	thin-layer chromatography

1. INTRODUCTION

DNA exonucleases are ubiquitous enzymes involved in a broad range of cellular processes. Primarily, exonucleases play a critical role in the maintenance of genomic material, as most DNA repair pathways rely on an exonuclease to excise damaged nucleotides (e.g., nucleotide excision repair, double-strand break (DSB) repair, base excision repair). Besides participating in DNA repair pathways, exonucleases are responsible for preventing mutagenesis by enhancing the fidelity of genomic replication. Many exonucleases act as proofreaders for replicative DNA polymerases, or take part in mismatch repair in the event that proofreading fails. As expected based on their central role in DNA metabolism, there are numerous diseases that are associated with mutations in exonuclease genes (Mason & Cox, 2012).

This chapter focuses on ensemble kinetic methods that have been used to characterize the exonuclease activity of the bacteriophage T4 MR complex. The MR complex, made up of the nuclease Mre11 and the ATPase Rad50, plays an important role in the initiation of DSB repair. DSBs can be caused by either physiological or pathological processes. Pathological DSBs are mainly caused by ionizing radiation and oxidative damage by cellular metabolites (Assenmacher & Hopfner, 2004; Chapman, Taylor, & Boulton, 2012; Deshpande, Lee, Arora, & Paull, 2016; Gobbini, Cassani, Villa, Bonetti, & Longhese, 2016; Lafrance-Vanasse, Williams, & Tainer, 2015). Defective DSB repair is a hallmark of many types of cancer and genotoxic chemicals that introduce DSBs are among the most commonly prescribed anticancer drugs (Broustas & Lieberman, 2014; Park, Chae, Kim, & Cho, 2011; Sung et al., 2014).

DSBs are repaired by one of two major pathways: homology-directed repair (HDR) and nonhomologous end joining. HDR involves extensive resection of 5′ strands, which is initiated by the Mre11/Rad50/Nbs1 complex in mammals, the Mre11/Rad50/Xrs2 in yeast, and the Mre11/Rad50

complex in bacteriophage T4. The resection begins with endonucleolytic cleavage of the DNA by Mre11. This creates a nick on the 5′ side of the DSB, which serves as an entry point for the 5′ to 3′ exonuclease Exo1 or Dna2 (Zhu, Chung, Shim, Lee, & Ira, 2008). The 5′ to 3′ exonuclease activity proceeding away from the DSB, combined with the 3′ to 5′ exonuclease activity of Mre11 proceeding toward the DSB, produces 3′ single-stranded DNA (ssDNA) that is then bound by the recombinase protein (Kakarougkas & Jeggo, 2014; Lammens et al., 2011; Li et al., 2017). In addition to its DSB repair functions, the T4 phage MR complex is responsible for degradation of host genomic DNA to fuel the T4 replisome with deoxynucleotides for phage DNA synthesis (Mickelson & Wiberg, 1981). This noncanonical function for the T4 MR complex may be the physiological reason for its more rapid ATPase and exonuclease activities when compared with other MR complexes (Deshpande, Lee, & Paull, 2017; Herdendorf, Albrecht, Benkovic, & Nelson, 2011).

The MR complex is a heterotetramer made up of two dimers each of Mre11 and Rad50. The nuclease activities of Mre11 reside in the core phosphodiesterase domain (Hopfner et al., 2001). Adjacent to this is a capping domain that aids in distinguishing between ssDNA and double-stranded DNA (dsDNA), and is thought to guide its orientation into the nuclease active site (Williams et al., 2008, p. 11). Rad50 belongs to the ABC ATPase superfamily and the structural maintenance of chromosome family (Hopfner, 2003, p. 50). The walker A and B motifs of the Rad50 dimer fold on themselves to form the ATPase active site. Antiparallel coiled coils extend from the globular domain and are linked at their ends through a zinc ion bound by a completely conserved CXXC motif (Lammens et al., 2011). Rad50 is a slow ATPase, but its activity is stimulated by Mre11 and DNA (Deshpande et al., 2017; Herdendorf et al., 2011). Likewise, Rad50 stimulates the exonuclease activity of Mre11 (Herdendorf et al., 2011; Lafrance-Vanasse et al., 2015).

The reaction kinetics of exonucleases may not follow conventional Michaelis–Menten kinetics due to their processivity (or lack thereof) on polymeric substrates. Processivity as it pertains to an exonuclease is the ability to remove multiple nucleotides in a single binding event and is essentially the probability of the enzyme carrying out another catalytic cycle rather than dissociate from its DNA substrate. Partial processivity may give rise to unusual kinetic phenomenon depending on the type of DNA substrate used and how products are monitored in the assay (Rentergent, Driscoll, & Hay, 2016). For example, the effects of low processivity can be either enhanced or

suppressed by adjusting the enzyme-to-substrate ratio. At a low enzyme-to-substrate ratio, a modifier or amino acid mutation that alters the processivity will have a larger effect than at a higher enzyme-to-substrate ratio. Additionally, the effects of processivity can be further modified by the type of the assay that is employed. In the commonly used fluorescence assay that relies on the removal of the modified nucleotide 2-aminopurine (2AP) from the substrate, the position of the label has a large effect on how a processivity modifier is perceived. Similarly, the polarity of the exonuclease can lead to nonlinearity with respect to enzyme concentration when using positional labels. These issues will be discussed in detail using our efforts to characterize the bacteriophage T4 MR complex as an example.

2. ASSAYS USING PLASMIDS AND PCR PRODUCTS

2.1 Agarose Gel Electrophoresis

The simplest exonuclease assays are based on agarose gel electrophoresis combined with a dye-based visualization (Koontz, 2013). These assays can be useful in determining the broad features of an exonuclease early in the characterization process (Trujillo, Yuan, Lee, & Sung, 1998). The DNA substrate for these assays is often a purified PCR product or a plasmid that has been linearized with a DNA restriction enzyme. Specific restriction enzymes can be chosen to provide either blunt DNA ends or 5′ or 3′ ssDNA overhangs. The linearized plasmid can also be treated with alkaline phosphatase to test the effect of removing the 5′ phosphate groups on the activity of the exonuclease. Similarly, with a PCR product, the primers used in the reaction can be synthesized with 5′ phosphates included or the PCR product can be phosphorylated using T4 polynucleotide kinase and ATP. The kinetic assays are stopped-time using EDTA as a quencher of the reaction and the agarose gels are ran in $1\times$ TAE or $0.5\times$ TBE buffer in the absence of intercalating dye. After the gel has ran, it is stained with ethidium bromide or other dsDNA-specific dye and destained if necessary. Often both the substrate and a smear of shorter products can be observed on a gel and the length of the shorter products may provide some information regarding the processivity of the exonuclease, depending on the time points taken and the enzyme-to-substrate ratio used. At this stage in the characterization process, it is important to confirm that the observed exonuclease activity originates from the enzyme under investigation and not a copurifying contaminating exonuclease. The most direct way to do this is to generate an active site mutant that is expected to greatly decrease the exonuclease

activity. For T4 Mre11, we mutated two residues (His^{10} and Asp^{48}) that were predicted to be necessary for binding the essential divalent cations and exonuclease activity was reduced to a value below our detection limit. If the exonuclease being investigated is endogenously expressed, or sites for mutations cannot be easily predicted, then it is recommended that the exonuclease activity be closely followed through several steps of purification to confirm that the elution profile of the protein of interest (visualized by SDS-PAGE) exactly matches elution profile of the observed exonuclease activity. The initial characterization of the T4 MR complex relied on a linearized pGEM plasmid that was used to determine that the exonuclease activity of T4 Mre11 depends on the presence of Rad50 and ATP and that it strongly prefers Mn^{2+} over Mg^{2+} or Zn^{2+} (Herdendorf et al., 2011; Fig. 1).

2.2 Alkaline Agarose Gel Electrophoresis

A more quantitative exonuclease assay that can be easily used to determine specific activities relies on the uniform labeling of a PCR product with [α-^{32}P] dNTPs (Herdendorf et al., 2011). In most cases, the label can be a single nucleotide (e.g., [α-^{32}P] dGTP) used in trace amounts relative to the unlabeled nucleotide. To avoid template-independent addition of dAMP to the 3′ end of the PCR product, a thymine should be used at

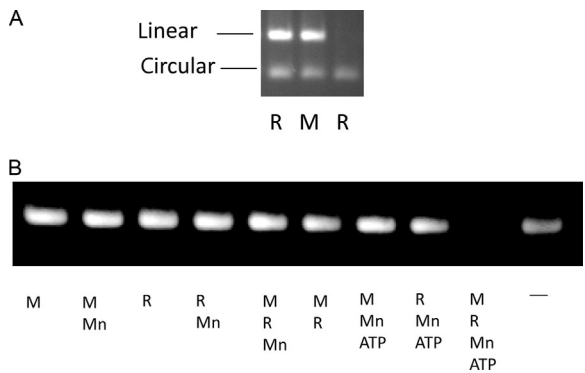

Fig. 1 Nuclease reactions visualized with TAE-agarose gels. (A) Reactions with 0.4 μg of circular and linearized forms of pGEM plasmid dsDNA using $MnCl_2$, Rad50 (R), Mre11 (M), and ATP concentrations of 5 m*M*, 300 n*M*, 300 n*M*, and 2 m*M*, respectively. (B) Reactions with 0.4 μg linearized pGEM dsDNA. The concentrations of $MnCl_2$ (Mn), Mre11 (M), Rad50 (R), and ATP were 5 m*M*, 300 n*M*, 300 n*M*, and 2 m*M*, respectively. *Panels were reproduced with permission from Herdendorf, T. J., Albrecht, D. W., Benkovic, S. J., & Nelson, S. W. (2011). Biochemical characterization of bacteriophage T4 Mre11-Rad50 complex.* Journal of Biological Chemistry, 286*(4), 2382–2392.* https://doi.org/10.1074/jbc.M110.178871.

the 5′ end of the primer (Brownstein, Carpten, & Smith, 1996), or the PCR should be carried out with a proofreading DNA polymerase that has minimal 3′ tailing activity. Again, if 5′ phosphates are desired, they can be incorporated into the PCR primers during synthesis or the purified PCR product can be phosphorylated with T4 polynucleotide kinase and ATP. The concentration of the radioactive purified PCR product is determined using liquid scintillation counting of a small aliquot of a diluted sample of the reaction before and after PCR fragment purification. Once the concentration of dGMP in the sample is determined (if [α-^{32}P] dGTP is used), the concentration of nucleotides is calculated using the %GC content of the amplified PCR product and the concentration of DNA ends is determined using the calculated molecular weight of the PCR fragment. The concentration of DNA ends is usually is submicromolar; therefore, the assays are normally performed using a high enzyme-to-DNA ratio so that the observed rates are independent of protein concentration (e.g., 200 n*M* protein with 20 n*M* DNA ends). Again, this is a stopped time reaction and the reaction products are separated using alkaline agarose electrophoresis (Sambrook & Russell, 2006). We typically use 0.8% agarose prepared and ran in 30 m*M* NaOH and 5 m*M* EDTA. After running for approximately 16 h, the gel is removed from its tray and neutralized by soaking for 1 h in 1 L of 1 × TBE buffer at room temperature. The neutralized gel is then dried onto a sheet of DE81 paper using a 2-in. stack of paper towels to facilitate gel drying. After 4 h of drying with the paper towels, the gel and filter sheet are vacuum-dried for 1 h and then exposed to a Phosphorimager screen. After scanning the screen, the substrate and products are quantitated using ImageJ or similar software (Schneider, Rasband, & Eliceiri, 2012).

2.3 Filter Binding and TLC Analysis

Filter binding and thin-layer chromatography (TLC) assays are more rapid methods for analyzing reactions carried out with labeled DNA. The uniformly labeled PCR product substrate (discussed in the previous section) produces ^{32}P-labeled dGMP as the product of the exonuclease reaction, which is easily separated from the much longer DNA substrate using a standard DNA DE81 filter binding assay (Brutlag & Kornberg, 1972) or TLC analysis using polyethyleneimine (PEI) cellulose plates (Merck Millipore) (Rajagopal & Lorsch, 2013). We prefer TLC analysis because of its ease of use, combined with its high accuracy and reproducibility, which is due to the simultaneous visualization of both substrates and products (Fig. 2A).

The total volume for these reactions can be quite low, on the order of a few microliters with only 0.5–1 μL used per time point. The plates are developed in 300 m*M* KPi, pH 6.8, air dried, and exposed to a Phosphorimager screen for 30–60 min. The screen is then imaged and the spots are quantitated and analyzed using ImageJ (Schneider et al., 2012) or similar software. Fig. 2A shows an exonuclease assay examining the effect of ATP on the activity on the MR complex using a [α-^{32}P] dGTP-labeled 1.9-kb PCR fragment. When adding nucleotides such as ATP, it is important to control for the stoichiometric binding of divalent cations by the nucleotide and adjust the concentration accordingly (to maintain a constant free cation concentration). Provided the exonuclease is specific for dsDNA, it is expected that at the

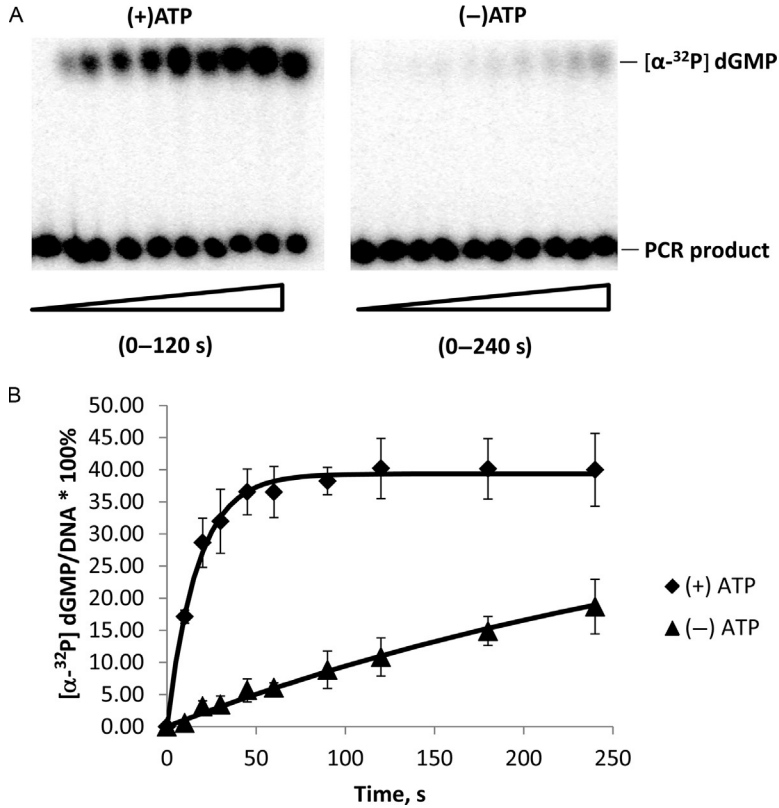

Fig. 2 TLC plate-based exonuclease assays. The DNA substrate is a 1.9-kb PCR product uniformly labeled with [α-^{32}P] dGMP. (A) The reaction contained 500 n*M* MR complex, 0.3 m*M* Mn^{2+}, and 5 m*M* Mg^{2+}. ATP, when present, was 2 m*M*. The degree of exonuclease activity in the presence or absence of ATP. The data were fit to a single-exponential equation.

completion of the reaction approximately half of the substrate will be degraded to mononucleotides. This is due to the exonuclease initiating from both ends and proceeding to remove nucleotides until they meet in the middle of the substrate, leaving half of the remaining DNA single stranded. The data points generated in the presence of ATP in Fig. 2B are well described by a single-exponential rise with a rate constant of $\sim 0.06\ s^{-1}$, which is then multiplied by half the number of bp in the DNA substrate (57 nts/s). In the absence of ATP, the observed exonuclease rate is much slower (2.6 nts/s), and an extended time course would be necessary to reach total substrate depletion. In this situation, rather than increasing the time of the assay, we increased the fitting accuracy of the single-exponential rate constant by fixing the amplitude of the exponential to that determined in the reaction performed in the presence of ATP (0.42).

Depending on the exonuclease under investigation, it may be possible to generate similar data as the uniformly ^{32}P-labeled DNA substrate assay using fluorescent dyes that specifically bind to dsDNA. Tolun and Myers have successfully employed a continuous fluorescent assay to monitor the reaction of several exonucleases (Tolun & Myers, 2003). These authors surveyed several commercially available dsDNA dyes that show a strong preference for dsDNA over ssDNA and do not strongly inhibit the exonuclease when bound to the DNA substrate. Most dyes inhibited exonuclease I, but it was found that low concentrations of PicoGreen did not inhibit the exonuclease and had a large difference in fluorescent yield when bound to dsDNA compared to ssDNA. This assay is convenient and produces high-quality exonuclease kinetics in real time; however, it must be optimized for each exonuclease under investigation, and in some cases PicoGreen may be inhibitory even at very low concentrations. For the T4 MR complex, which is a moderately processive 3′ to 5′ exonuclease, we were unable to find conditions where the PicoGreen did not significantly reduce the exonuclease activity compared to the ^{32}P-based assay described earlier.

3. END-LABELED OLIGONUCLEOTIDE SUBSTRATES

The resolution and ability to quantitate DNA using agarose gels is limited; therefore, when direct observation of the DNA substrate and products is beneficial, it is more common to use denaturing polyacrylamide gel electrophoresis (urea-PAGE) with short end-labeled oligonucleotides that can be synthesized by a commercial vendor (Albrecht, Herdendorf, & Nelson, 2012). The sequences of the oligonucleotides are under the

complete control of the investigator and they can be easy labeled at the 3′ or 5′ ends with fluorescent dyes during synthesis (Kricka, 2002). As with any modification of a substrate, control experiments must be performed to ensure that the attached fluorescent label does not reduce activity. It is not uncommon for proteins to have affinity for the attached dyes, which lowers the effective enzyme concentration. To determine if an enzyme has affinity for an appended dye, a fluorescence anisotropy assay can be used to determine the binding constants for the modified DNA and an unmodified DNA competitor (Heyduk, Ma, Tang, & Ebright, 1996). If it is determined that the enzyme has affinity for fluorescent dyes or increased detection sensitivity is required, 5′-^{32}P end labeling can be performed using T4 polynucleotide kinase and [γ-^{32}P] ATP. The oligonucleotide can be labeled as ssDNA, then annealed to its complementary strand or the complementary strands can be annealed prior to the PNK reaction. 3′-^{32}P labeling requires the incorporation of a [α-^{32}P] dNTP using a DNA polymerase. In this case, the complementary strands need to be designed to leave a single nucleotide 5′ overhang that will be filled in using the appropriate ^{32}P nucleotide. A proofreading-deficient DNA polymerase should be used and the DNA should be designed in such a way to avoid the use of dATP or dGTP, as many DNA polymerases that lack exonuclease activity will incorporate these nucleotides in a template-independent manner to make a single nucleotide 5′ overhang (Fiala et al., 2007).

Special care should be taken in the sequence design for oligonucleotide-based exonuclease substrates. DNA sequences with the potential to form intramolecular hairpins and intermolecular dimers should be avoided. The activity of some exonucleases is dependent on the %GC content of their substrates, with higher GC leading to a slower exonuclease activity (van Oijen et al., 2003). This type of dependence suggests that melting of the basepair either prior to or after the exonucleolytic cut is at least partially rate-limiting under the conditions of the assay. It is therefore important to control the global %GC content of the substrate. If nothing is known regarding the GC dependence beforehand, the DNA substrate should be designed to match the %GC content of the organism in which it resides. Because the T4 MR complex is responsible for degrading the *Escherichia coli* genome (~50% GC) and acting on the bacteriophage T4 genome (34.5% GC), we have systematically examined the dependence of T4 MR complex on the %GC of the substrate (Teklemariam, unpublished observations). Surprisingly, we found that DNA sequences with a higher %GC content are better substrates for the T4 MR complex. We also found that transitions

between high and low GC tend to act as stall sites (e.g., a stretch of G/Cs followed by several Ts), highlighting the importance of controlling the local DNA sequence as well.

Depending on the length of the oligonucleotides used, it may be possible to directly determine the processivity of the exonuclease by a visual examination of the gel, or at a minimum, put a limit on its value (Subramanian, Rutvisuttinunt, Scott, & Myers, 2003). As an example, Fig. 3 shows an exonuclease reaction using a 50 bp dsDNA substrate that is labeled at both 5′ ends with hexachlorofluorescein dye. Initially, several different fluorescent dyes were tested and their activity was compared to 5′ ^{32}P-labeled DNA substrate. We found that both Cy3- and Cy5-labeled substrates displayed lower activity compared to the ^{32}P-labeled substrate, suggesting that the MR complex was directly binding to these labels. Additionally, charged dyes

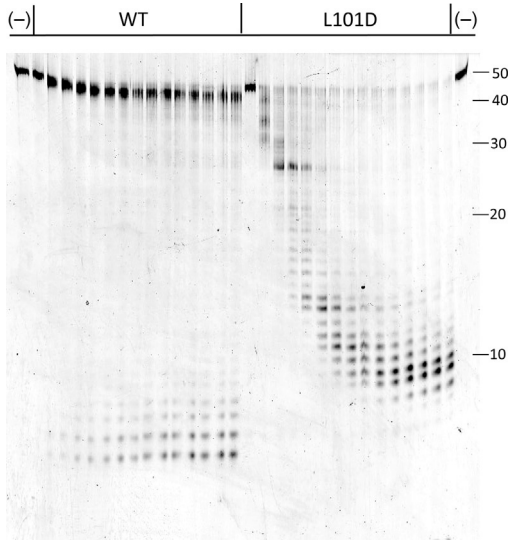

Fig. 3 Example of a processive (WT) and nonprocessive (L101D) exonuclease reactions. The products are visualized on 16% urea-polyacrylamide gel. Each assay consisted of 0.3 m*M* $MnCl_2$, 100 n*M* Rad50, 105 n*M* Mre11, 2 m*M* ATP, and 1.3 μ*M* DNA substrate. Time points vary from 0 to 120 min. The *first* and *last lanes* are no protein controls and the approximate mobility of various DNA lengths is shown on the *right-hand side* of the gel. *Figure was reproduced with permission from Albrecht, D. W., Herdendorf, T. J., & Nelson, S. W. (2012). Disruption of the bacteriophage T4 Mre11 dimer interface reveals a two-state mechanism for exonuclease activity.* Journal of Biological Chemistry, 287*(37), 31371–31381. https://doi.org/10.1074/jbc.M112.392316*.

such as Cy3 and Cy5 should be avoided if possible, as they display aberrant migration patterns during electrophoresis when attached to oligonucleotides shorter than eight nucleotides (Killelea, Saint-Pierre, Ralec, Gasparutto, & Henneke, 2014). Fluorescein and hexachlorofluorescein were not inhibitory; therefore, hexachlorofluorescein was chosen due to its increased stability compared to fluorescein. The reactions shown in Fig. 3 were performed with a low enzyme-to-DNA ratio in the presence of ATP, so that at early time points the probability of binding to an intermediate product is minimal (referred to as "single-hit" conditions). Under these conditions, the product profile is a direct reporter of processivity (Bambara, Fay, & Mallaber, 1995). The exonuclease reaction carried out with a mutant MR complex that has a disrupted Mre11 dimer interface (L101D) indicates that the mutant has rendered the MR complex nonprocessive, as a progressive decrease in product length is seen as time increases. The ATP-dependent reaction using the wild-type MR complex does not exhibit this progressive decrease and only very short products are observed; therefore, the processivity in the presence of ATP is at least as long as the DNA substrate (50 bp) (Albrecht et al., 2012).

While determining processivity by direct visualization of the products under "single-hit" provides a good estimate of processivity, it may be preferable to determine the rate constants for forward translocation/exonuclease activity and product dissociation. Determining the rate constants for these steps in the catalytic cycle may be accomplished by global fitting of full progress curves using DNA substrates containing a 2AP probe located in at least two positions along the DNA substrate (the 2AP probe is discussed in detail in Section 5). Shown in Fig. 4 is an example of progress curve analysis of the MR complex acting on a 50 bp DNA substrate with 2AP probes located at the first and eight positions. The software DynaFit was used to numerically integrate a simple mechanism that includes association and dissociation rate constants for enzyme and DNA and a single combined rate constant for the translocation/exonuclease step (k_{exo}) (Kuzmic, 2009; Reytor González, Cornell-Kennon, Schaefer, & Kuzmič, 2017). Processivity can be defined by the probability that the exonuclease performs another round of nucleotide removal instead of dissociating from the DNA (processivity $= k_{exo}/(k_{exo} + k2)$). The processivity of the MR complex under the conditions of this experiment (the absence of ATP) is 0.55, indicating that the enzyme has almost an equal probability of undergoing another round of catalysis as it does falling off the DNA, consistent with what has been observed using urea-PAGE analysis.

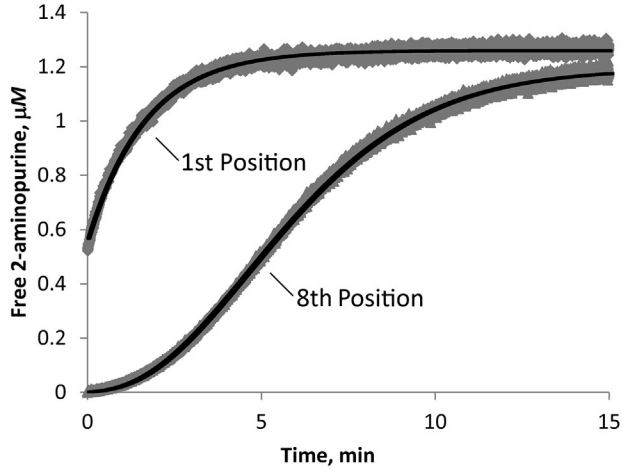

$$E + DNA_{50} \Leftrightarrow EDNA_{50} \quad : k1\ k2$$
$$EDNA_{50} \rightarrow EDNA_{49} + P \quad : k_{exo}$$
$$EDNA_{49} \Leftrightarrow E + DNA_{49} \quad : k2\ k1$$
$$EDNA_{50} \rightarrow EDNA_{49} + X \quad : k_{exo}$$
$$\downarrow$$
$$EDNA_{43} \rightarrow EDNA_{42} + Q \quad : k_{exo}$$
$$EDNA_{42} \Leftrightarrow E + DNA_{42} \quad : k2\ k1$$
$$\downarrow$$
$$EDNA_{1} \rightarrow E + X \quad : k_{exo}$$

Fig. 4 Global fitting of full progress curves with the 2-aminopurine probe in either the first and eight positions. The *gray points* and *black lines* represent the experimental data and the theoretical fits, respectively. The reactions were carried out in the absence of ATP with 400 n*M* MR complex and 1.3 μ*M* 50 bp DNA substrate. The data were fit with the DynaFit program using the mechanism shown. The association rate (*k*1) was fixed at 50 $\mu M^{-1}\ s^{-1}$ and *k*2 and k_{exo} were determined to be 2.68 ± 0.05 and $3.28 \pm 0.03\ min^{-1}$.

4. DETERMINING EXONUCLEASE POLARITY

The polarity of an exonuclease can be determined using several different biochemical assays. A straightforward method is separately ^{32}P label a long DNA substrate (100–1000 bp, often a PCR product) at the 3′ and 5′ ends and follow the time course of the exonuclease reaction using a DE81-filter binding, PEI cellulose TLC, or urea-PAGE (Herdendorf et al., 2011; Trujillo & Sung, 2001). Labeling the 5′ end is carried out using T4 PNK and [γ-^{32}P] ATP, whereas labeling of the 3′ end is performed in two steps. In the first step, the terminal 3′ nucleotide is removed using a

proofreading polymerase. The DNA sequence of the PCR primers must be chosen so that only a single nucleotide is removed by the proofreading polymerase (e.g., wild-type T4 DNA polymerase) when a specific deoxynucleotide is included in the reaction. For example, if a primer with the sequence 5′-AGACGTAGCGTATCGCAGGC is used, then a high concentration of dCTP (1–5 m*M*) should be included in the reaction to ensure that only the terminal 3′ nucleotide is removed by the polymerase. After a brief incubation with the polymerase (~10 min at 37°C), the reaction is purified using phenol/chloroform extraction or commercial PCR clean up kit (the dCTP must be removed to avoid misincorporation in the next step). Next, an exonuclease-deficient DNA polymerase is added to the reaction, along with [α-^{32}P] dTTP. After 10 min, 50 μ*M* unlabeled dTTP is added and the reaction is allowed to proceed for 10 additional minutes, followed by purification of the product. The DNA concentration is determined using scintillation counting as described earlier, except it is assumed that only two ^{32}P labels per substrate are incorporated. If the end-labeled DNA used for the exonuclease assay is sufficiently long, then there will be a delay in the formation of the mononucleotide product on the end distal from the initiating end. In some cases, only a single type of end label will produce a labeled nucleotide monophosphate product because the complementary strands will melt as the exonuclease approaches the end of the substrate. This produces labeled ssDNA approximately 5–10 bases long that binds to DE81 filter paper or PEI cellulose in a similar fashion as the substrate.

If the reaction products are visualized using urea-PAGE, then the product profile often immediately suggests the polarity of the reaction. The T4 MR complex is a 3′ to 5′ exonuclease and the product pattern it produces is shown in Fig. 5. However, with highly active and processive exonucleases, it may be difficult to observe reaction intermediates that would normally be present when the enzyme initiates on the end distal to the label. In this situation, it is advantageous to employ 5′- and 3′-labeled oligonucleotide DNA substrates in combination with thiophosphoryl linkages at either end of the DNA. The activity of most exonucleases (including Mre11) is inhibited by thiophosphoryl groups. The thiophosphoryl groups enable the use of small oligonucleotide substrates and rapid analysis of the reaction via filter binding or PEI cellulose TLC. We examined the exonuclease activity of T4 MR by PEI cellulose TLC using four individual substrates (Fig. 6). Only the thiophosphoryl linkage at the 3′ position inhibits the production of the ^{32}P-labeled mononucleotide, consistent with a 3′ to 5′ exonuclease.

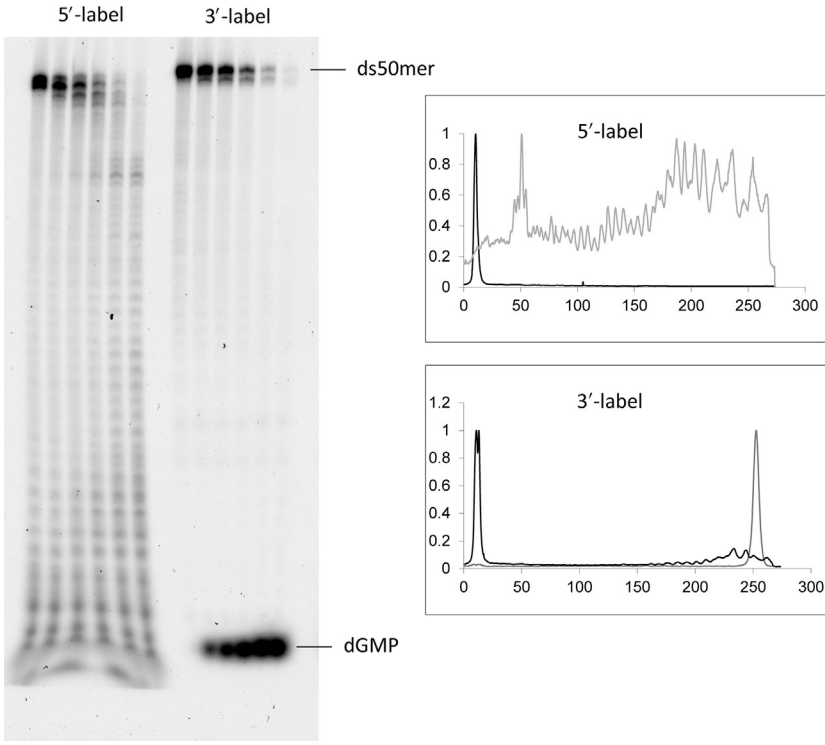

Fig. 5 Analysis of the polarity of nuclease activity using 16% urea-PAGE. The reaction was carried out at 37°C, and the time points for each lane are 0, 0.5, 1, 2, 4, and 8 min. The concentrations of dsDNA, Mre11, Rad50, $MnCl_2$, and ATP were 0.5 μ*M*, 100 n*M*, 100 n*M*, 5 m*M*, and 2 m*M*, respectively. *Figure was reproduced with permission from Herdendorf, T. J., Albrecht, D. W., Benkovic, S. J., & Nelson, S. W. (2011). Biochemical characterization of bacteriophage T4 Mre11-Rad50 complex.* Journal of Biological Chemistry, *286(4), 2382–2392. https://doi.org/10.1074/jbc.M110.178871*.

5. 2-AMINOPURINE-BASED OLIGONUCLEOTIDE SUBSTRATES

Perhaps the most convenient and informative exonuclease assays are based on the fluorescent base analog 2AP. The fluorescence of 2AP is quenched through base-stacking interactions so that when it is removed by the exonuclease, its fluorescent emission greatly increases (Frey, Sowers, Millar, & Benkovic, 1995; Jean & Hall, 2001). The 2AP base has been extensively used to indirectly report on the conformational changes that occur within the enzyme active site during the exonuclease reaction

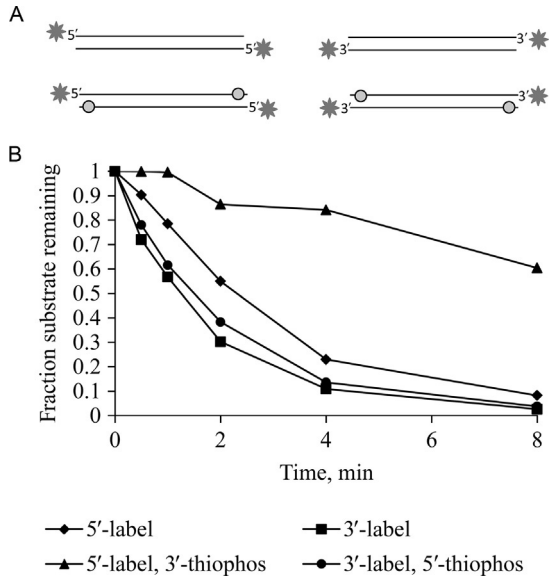

Fig. 6 TLC-based assay for determination of exonuclease polarity. (A) Four DNA substrates utilized to determine exonuclease polarity. The ^{32}P labels and thiophosphoryl groups are represented by the *gray stars* and *circles*, respectively. (B) Quantification of an exonuclease reaction carried out in the absence of ATP with 50 n*M* MR complex and 1.3 μ*M* DNA substrate.

and the kinetics of exonucleolytic removal of the base itself (Bloom et al., 1994; Frey et al., 1995). A major advantage of 2AP is that it can be easily incorporated into well-defined DNA substrates via oligonucleotide synthesis by several commercial vendors. The 2AP probe can be placed at any internal site or at the 3′ or 5′ end of the oligonucleotide. For determining simple comparative exonuclease activities, we incorporate the 2AP probe at the 3′ end and refer to this as the first position. We have also used the first position 2AP DNA substrate to perform traditional steady-state kinetics under multiple turnover conditions to determine the kinetic constants and binding order of DNA and either Mg^{2+} or Mn^{2+} as a coactivator. In this case, we included a thiophosphoryl linkage between the second and third position of the substrate so that the MR complex dissociates from the DNA substrate rather than removing multiple nucleotides in a processive fashion. Steady-state nuclease assays were performed where the concentrations of DNA substrate and coactivating metal were varied at concentrations above and below their apparent affinity constants (Fig. 7). The initial

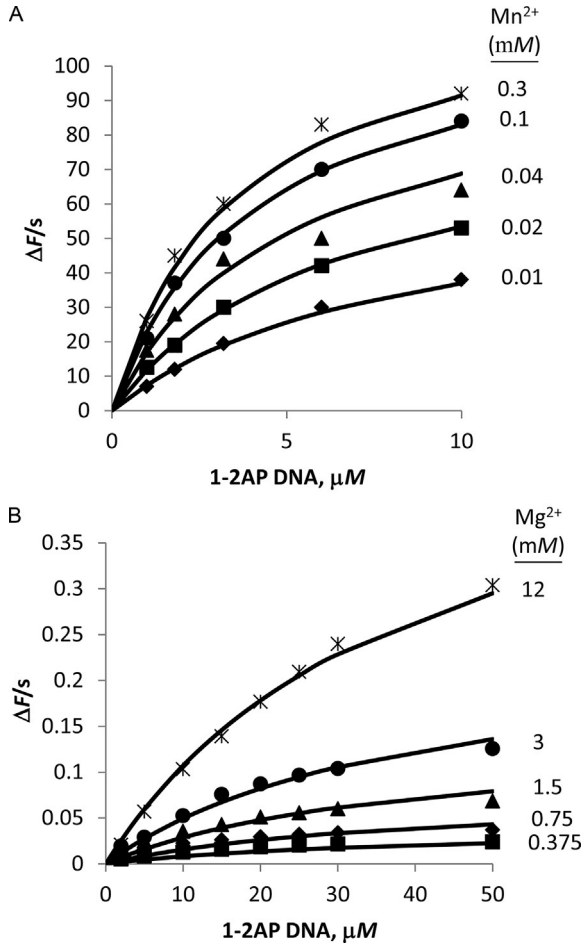

Fig. 7 Kinetic mechanism of T4 MR complex excising a 2-aminopurine nucleotide from the first position in the presence of Mn^{2+} (A) or Mg^{2+} (B). Reactions were performed in the absence of ATP with 50 n*M* MR complex. The data were fit to a rapid equilibrium random mechanism and the determined values are found in Table 1.

velocities were determined from the linear portion of each time course and the data were fit to four possible models using DynaFit software (BioKin Ltd.) (Kuzmic, 2009). In this analysis, DNA and the divalent metal cation are considered a substrate and an essential activator, respectively. The four models tested under the rapid equilibrium approximation were: (1) ordered addition with DNA binding first; (2) ordered addition with Mg^{2+} binding first; (3) random addition with different affinities for the free and substrate-/activator-bound form of the enzyme; and (4) random addition with identical

affinities for the free and substrate-/activator-bound form of the enzyme (Segel, 1975). When Mg^{2+} is the activating metal, the statistical analysis indicated that the most plausible model is a random addition with identical affinities for the free enzyme and the single-substrate-/activator-bound form (Table 1). On the other hand, synergy is observed between the binding of Mn^{2+} and the DNA substrate such that the affinity for DNA binding to the Mn^{2+}-bound enzyme is threefold higher than in its absence (Table 1). The turnover number (k_{cat}-Mn^{2+}) was 57 s^{-1}, or about 65-fold higher than the Mg^{2+}-catalyzed reaction (Table 1).

The activity of the T4 MR complex using the first position 2AP DNA without the thiophosphoryl linkage as a substrate provided a hint that the complex might increase in processivity in the presence of ATP. On the basis of the gel-based assays that were previously performed, it was clear that ATP is a strong activator of T4 MR complex; however, using the first position substrate under multiple turnover conditions ([E] ≫ [DNA]), ATP became inhibitory. The simplest explanation for this observation is that ATP slows product dissociation. This could result from either a slow release of the $n-1$ product or from processive translocation/exonuclease activity of the complex along the DNA substrate, which prevents the enzyme from dissociating and rebinding to another DNA substrate. To distinguish between these possibilities, the 2AP probe can be moved to an internal site located some distance away from the DNA end. In the case of T4 MR complex, the observed exonuclease activity decreases relative to the first position 2AP and the presence of ATP now becomes strongly activating. As shown in Fig. 8A, the ratio of activities in the presence and absence of ATP increases

Table 1 Steady-State Kinetic Parameters for T4 MR Complex Exonuclease Activity

	Activating Metal	
Parameter	**Mg^{2+} (μ*M*)**	**Mn^{2+} Value (μ*M*)**
K_{ia}[a]	7700 ± 600	37 ± 7
K_{im}[b]	39 ± 4	10 ± 4
K_a[c]	7700 ± 600	11 ± 3
K_m[d]	39 ± 4	3.2 ± 0.4
k_{cat}	0.9 ± 0.1	56 ± 2

[a] K_{ia} is the dissociation constant for $E + Mx^{2+} \Leftrightarrow E - Mx^{2+}$, where Mx^{2+} is Mg^{2+} or Mn^{2+}.
[b] K_{im} is the dissociation constant for $E + DNA \Leftrightarrow E - DNA$.
[c] K_a is the dissociation constant for $E - DNA + Mx^{2+} \Leftrightarrow E - DNA - Mx^{2+}$, where Mx^{2+} is Mg^{2+} or Mn^{2+}.
[d] K_m is the dissociation constant for $E - Mx^{2+} + DNA \Leftrightarrow E - DNA - Mx^{2+}$.

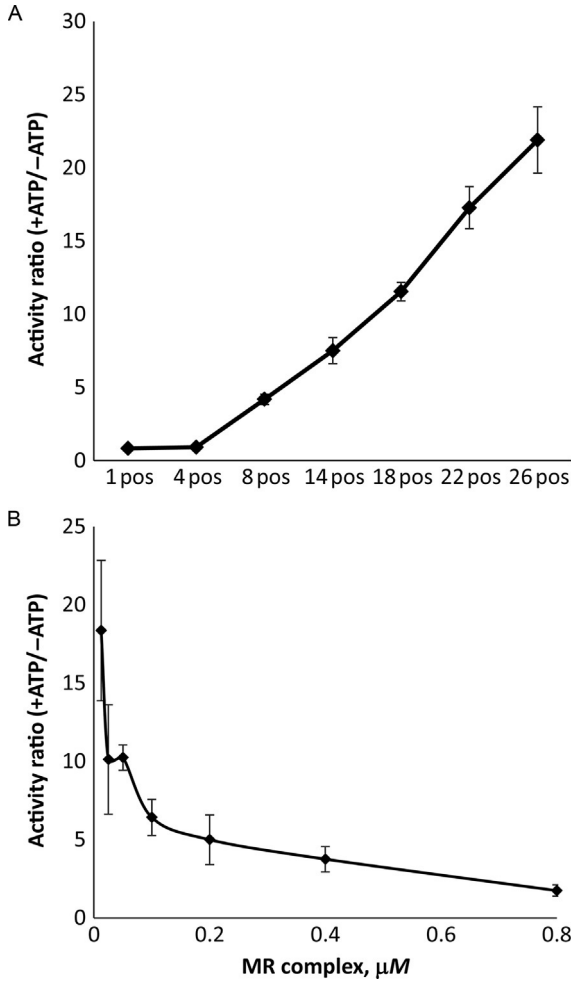

Fig. 8 Effect of ATP on the processivity of the T4 MR complex. (A) The ratio of the exonuclease activity in the presence and absence of ATP with the 2-aminopurine probe located at the positions indicated on the *x*-axis. The concentration of the MR complex was held at 50 n*M*. (B) The ratio of the exonuclease activity in the presence and absence of ATP at various concentrations of the MR complex with the 2-aminopurine probe located at the 18th position. For both (A) and (B), the concentrations of dsDNA, $MnCl_2$, $MgCl_2$, and ATP (when present) were 1.3 μ*M*, 0.3 m*M*, 5 m*M*, and 2 m*M*, respectively.

as the 2AP probe is moved away from the initiating 3′ end of the DNA. This strongly suggests that ATP increases the activity of the MR complex by increasing its processivity. Consistent with the presence of processivity, when using a single internal 2AP at the 18th position, the activating effect

of ATP diminishes as the concentration of enzyme increases (Fig. 8B). Qualitatively, these data indicate that the T4 MR complex by itself has very limited processivity and that Rad50 enhances it through its ATPase activity.

6. CONCLUSIONS

Exonucleases play a vital role in maintaining the integrity of genomic DNA by participating in nearly all DNA repair pathways and by acting as proofreaders to increase the fidelity of DNA synthesis. Similar to DNA polymerases, there are a wide variety of activity assays that can be used to characterize the activity of DNA exonucleases. The ensemble assays presented here have been valuable tools in the characterization of the T4 MR complex and can easily be applied to most other DNA exonucleases. The T4 MR complex is a Mn^{2+}-dependent, ATP-activated 3′ to 5′ exonuclease. The primary effect of ATP binding and hydrolysis is to increase the processivity of the complex as it translocates along its DNA substrate. The assays described here can be used to characterize the effects of site-directed mutations or interaction with potential binding partners on DNA affinity, exonuclease rate, and processivity. The assays employing 2AP could easily be adapted to high-throughput format for the identification of inhibitors that could serve as potential drug candidates. DNA repair pathways are often upregulated in tumor cells treated with DNA-damaging agents and inhibition of specific exonucleases sensitizes cells to these agents (Chang et al., 2016; Rajecki et al., 2009; Wang et al., 2017; Xu et al., 2004).

REFERENCES

Albrecht, D. W., Herdendorf, T. J., & Nelson, S. W. (2012). Disruption of the bacteriophage T4 Mre11 dimer interface reveals a two-state mechanism for exonuclease activity. *The Journal of Biological Chemistry*, *287*(37), 31371–31381. https://doi.org/10.1074/jbc.M112.392316.

Assenmacher, N., & Hopfner, K. P. (2004). MRE11/RAD50/NBS1: Complex activities. *Chromosoma*, *113*(4), 157–166. https://doi.org/10.1007/s00412-004-0306-4.

Bambara, R. A., Fay, P. J., & Mallaber, L. M. (1995). Methods of analyzing processivity. *Methods in Enzymology*, *262*, 270–280.

Bloom, L. B., Otto, M. R., Eritja, R., Reha-Krantz, L. J., Goodman, M. F., & Beechem, J. M. (1994). Pre-steady-state kinetic analysis of sequence-dependent nucleotide excision by the 3′-exonuclease activity of bacteriophage T4 DNA polymerase. *Biochemistry*, *33*(24), 7576–7586.

Broustas, C. G., & Lieberman, H. B. (2014). DNA damage response genes and the development of cancer metastasis. *Radiation Research*, *181*(2), 111–130. https://doi.org/10.1667/RR13515.1.

Brownstein, M. J., Carpten, J. D., & Smith, J. R. (1996). Modulation of non-templated nucleotide addition by Taq DNA polymerase: Primer modifications that facilitate genotyping. *BioTechniques*, *20*(6), 1004–1006. 1008–1010.

Brutlag, D., & Kornberg, A. (1972). Enzymatic synthesis of deoxyribonucleic acid. 36. A proofreading function for the 3′ leads to 5′ exonuclease activity in deoxyribonucleic acid polymerases. *The Journal of Biological Chemistry*, *247*(1), 241–248.

Chang, L., Huang, J., Wang, K., Li, J., Yan, R., Zhu, L., et al. (2016). Targeting Rad50 sensitizes human nasopharyngeal carcinoma cells to radiotherapy. *BMC Cancer*, *16*, 190. https://doi.org/10.1186/s12885-016-2190-8.

Chapman, J. R., Taylor, M. R. G., & Boulton, S. J. (2012). Playing the end game: DNA double-strand break repair pathway choice. *Molecular Cell*, *47*(4), 497–510. https://doi.org/10.1016/j.molcel.2012.07.029.

Deshpande, R. A., Lee, J. H., Arora, S., & Paull, T. T. (2016). Nbs1 converts the human Mre11/Rad50 nuclease complex into an endo/exonuclease machine specific for protein-DNA adducts. *Molecular Cell*, *64*(3), 593–606. https://doi.org/10.1016/j.molcel.2016.10.010.

Deshpande, R. A., Lee, J.-H., & Paull, T. T. (2017). Rad50 ATPase activity is regulated by DNA ends and requires coordination of both active sites. *Nucleic Acids Research*, *45*(9), 5255–5268. https://doi.org/10.1093/nar/gkx173.

Fiala, K. A., Brown, J. A., Ling, H., Kshetry, A. K., Zhang, J., Taylor, J.-S., et al. (2007). Mechanism of template-independent nucleotide incorporation catalyzed by a template-dependent DNA polymerase. *Journal of Molecular Biology*, *365*(3), 590–602. https://doi.org/10.1016/j.jmb.2006.10.008.

Frey, M. W., Sowers, L. C., Millar, D. P., & Benkovic, S. J. (1995). The nucleotide analog 2-aminopurine as a spectroscopic probe of nucleotide incorporation by the Klenow fragment of Escherichia coli polymerase I and bacteriophage T4 DNA polymerase. *Biochemistry*, *34*(28), 9185–9192.

Gobbini, E., Cassani, C., Villa, M., Bonetti, D., & Longhese, M. (2016). Functions and regulation of the MRX complex at DNA double-strand breaks. *Microbial Cell*, *3*(8), 329–337. https://doi.org/10.15698/mic2016.08.517.

Herdendorf, T. J., Albrecht, D. W., Benkovic, S. J., & Nelson, S. W. (2011). Biochemical characterization of bacteriophage T4 Mre11-Rad50 complex. *The Journal of Biological Chemistry*, *286*(4), 2382–2392. https://doi.org/10.1074/jbc.M110.178871.

Heyduk, T., Ma, Y., Tang, H., & Ebright, R. H. (1996). Fluorescence anisotropy: Rapid, quantitative assay for protein-DNA and protein-protein interaction. *Methods in Enzymology*, *274*, 492–503.

Hopfner, K. (2003). Rad50/SMC proteins and ABC transporters: Unifying concepts from high-resolution structures. *Current Opinion in Structural Biology*, *13*, 249–255. https://doi.org/10.1016/S0959-440X(03)00037-X.

Hopfner, K. P., Karcher, A., Craig, L., Woo, T. T., Carney, J. P., & Tainer, J. A. (2001). Structural biochemistry and interaction architecture of the DNA double-strand break repair Mre11 nuclease and Rad50-ATPase. *Cell*, *105*(4), 473–485.

Jean, J. M., & Hall, K. B. (2001). 2-Aminopurine fluorescence quenching and lifetimes: Role of base stacking. *Proceedings of the National Academy of Sciences of the United States of America*, *98*(1), 37–41. https://doi.org/10.1073/pnas.011442198.

Kakarougkas, A., & Jeggo, P. A. (2014). DNA DSB repair pathway choice: An orchestrated handover mechanism. *British Journal of Radiology*, *87*(1035). https://doi.org/10.1259/bjr.20130685.

Killelea, T., Saint-Pierre, C., Ralec, C., Gasparutto, D., & Henneke, G. (2014). Anomalous electrophoretic migration of short oligodeoxynucleotides labelled with 5′-terminal Cy5 dyes. *Electrophoresis*, *35*(14), 1938–1946. https://doi.org/10.1002/elps.201400018.

Koontz, L. (2013). Agarose gel electrophoresis. *Methods in Enzymology*, *529*, 35–45. https://doi.org/10.1016/B978-0-12-418687-3.00004-5.

Kricka, L. J. (2002). Stains, labels and detection strategies for nucleic acids assays. *Annals of Clinical Biochemistry*, *39*(Pt. 2), 114–129. https://doi.org/10.1258/0004563021901865.

Kuzmic, P. (2009). DynaFit—A software package for enzymology. *Methods in Enzymology*, *467*, 247–280. https://doi.org/10.1016/S0076-6879(09)67010-5.

Lafrance-Vanasse, J., Williams, G. J., & Tainer, J. A. (2015). Envisioning the dynamics and flexibility of Mre11-Rad50-Nbs1 complex to decipher its roles in DNA replication and repair. *Progress in Biophysics and Molecular Biology*, *117*(2–3), 182–193. https://doi.org/10.1016/j.pbiomolbio.2014.12.004.

Lammens, K., Bemeleit, D. J., Möckel, C., Clausing, E., Schele, A., Hartung, S., et al. (2011). The Mre11:Rad50 structure shows an ATP dependent molecular clamp in DNA double-strand break repair. *Cell*, *145*(1), 54–66. https://doi.org/10.1016/j.cell.2011.02.038.

Li, Y., Wang, J., Zhou, G., Lajeunesse, M., Le, N., Stawicki, B. N., et al. (2017). Nonhomologous end-joining with minimal sequence loss is promoted by the Mre11-Rad50-Nbs1-Ctp1 complex in Schizosaccharomyces pombe. *Genetics*, *206*(1), 481–496.

Mason, P. A., & Cox, L. S. (2012). The role of DNA exonucleases in protecting genome stability and their impact on ageing. *Age*, *34*(6), 1317–1340. https://doi.org/10.1007/s11357-011-9306-5.

Mickelson, C., & Wiberg, J. S. (1981). Membrane-associated DNase activity controlled by genes 46 and 47 of bacteriophage T4D and elevated DNase activity associated with the T4 das mutation. *Journal of Virology*, *40*(1), 65–77.

Park, Y. B., Chae, J., Kim, Y. C., & Cho, Y. (2011). Crystal structure of human Mre11: Understanding tumorigenic mutations. *Structure*, *19*(11), 1591–1602. https://doi.org/10.1016/j.str.2011.09.010.

Rajagopal, V., & Lorsch, J. R. (2013). ATP and GTP hydrolysis assays (TLC). *Methods in Enzymology*, *533*, 325–334. https://doi.org/10.1016/B978-0-12-420067-8.00025-8.

Rajecki, M., af Hallstrom, T., Hakkarainen, T., Nokisalmi, P., Hautaniemi, S., Nieminen, A. I., et al. (2009). Mre11 inhibition by oncolytic adenovirus associates with autophagy and underlies synergy with ionizing radiation. *International Journal of Cancer*, *125*(10), 2441–2449.

Rentergent, J., Driscoll, M. D., & Hay, S. (2016). Time course analysis of enzyme-catalyzed DNA polymerization. *Biochemistry*, *55*(39), 5622–5634. https://doi.org/10.1021/acs.biochem.6b00442.

Reytor González, M. L., Cornell-Kennon, S., Schaefer, E., & Kuzmič, P. (2017). An algebraic model to determine substrate kinetic parameters by global nonlinear fit of progress curves. *Analytical Biochemistry*, *518*, 16–24. https://doi.org/10.1016/j.ab.2016.11.001.

Sambrook, J., & Russell, D. W. (2006). Alkaline agarose gel electrophoresis. *CSH Protocols*, *1*, 2006.

Schneider, C. A., Rasband, W. S., & Eliceiri, K. W. (2012). NIH image to ImageJ: 25 years of image analysis. *Nature Methods*, *9*(7), 671–675.

Segel, I. H. (1975). Rapid equilibrium bireactant and terreactant systems. In *Enzyme kinetics* (pp. 273–345). New York: John Wiley & Sons.

Subramanian, K., Rutvisuttinunt, W., Scott, W., & Myers, R. S. (2003). The enzymatic basis of processivity in lambda exonuclease. *Nucleic Acids Research*, *31*(6), 1585–1596.

Sung, S., Li, F., Park, Y. B., Kim, J. S., Kim, A.-K., Song, O.-K., et al. (2014). DNA end recognition by the Mre11 nuclease dimer: Insights into resection and repair of damaged DNA. *The EMBO Journal*, *33*(20), 1–14. https://doi.org/10.15252/embj.201488299.

Tolun, G., & Myers, R. S. (2003). A real-time DNase assay (ReDA) based on PicoGreen fluorescence. *Nucleic Acids Research*, *31*(18), e111.

Trujillo, K. M., & Sung, P. (2001). DNA structure-specific nuclease activities in the Saccharomyces cerevisiae Rad50*Mre11 complex. *The Journal of Biological Chemistry*, *276*(38), 35458–35464. https://doi.org/10.1074/jbc.M105482200.

Trujillo, K. M., Yuan, S. S., Lee, E. Y., & Sung, P. (1998). Nuclease activities in a complex of human recombination and DNA repair factors Rad50, Mre11, and p95. *The Journal of Biological Chemistry*, *273*(34), 21447–21450. https://doi.org/10.1074/jbc.273.34.21447.

van Oijen, A. M., Blainey, P. C., Crampton, D. J., Richardson, C. C., Ellenberger, T., & Xie, X. S. (2003). Single-molecule kinetics of lambda exonuclease reveal base dependence and dynamic disorder. *Science (New York, N.Y.)*, *301*(5637), 1235–1238. https://doi.org/10.1126/science.1084387.

Wang, Y., Gudikote, J., Giri, U., Yan, J., Deng, W., Ye, R., et al. (2017). RAD50 expression is associated with poor clinical outcomes after radiotherapy for resected non-small cell lung cancer. *Clinical Cancer Research: An Official Journal of the American Association for Cancer Research*, *24*, 341–350. https://doi.org/10.1158/1078-0432.CCR-17-1455.

Williams, R. S., Moncalian, G., Williams, J. S., Yamada, Y., Limbo, O., Shin, D. S., et al. (2008). Mre11 dimers coordinate DNA end bridging and nuclease processing in double-strand-break repair. *Cell*, *135*(1), 97–109. https://doi.org/10.1016/j.cell.2008.08.017.

Xu, M., Myerson, R. J., Hunt, C., Kumar, S., Moros, E. G., Straube, W. L., et al. (2004). Transfection of human tumour cells with Mre11 siRNA and the increase in radiation sensitivity and the reduction in heat-induced radiosensitization. *International Journal of Hyperthermia: The Official Journal of European Society for Hyperthermic Oncology, North American Hyperthermia Group*, *20*(2), 157–162.

Zhu, Z., Chung, W., Shim, E., Lee, S., & Ira, G. (2008). Sgs1 helicase and two nucleases Dna2 and Exo1 resect DNA double-strand break ends. *Cell*, *134*(6), 981–994. https://doi.org/10.1016/j.cell.2008.08.037.